Multiphoton Interference in Quantum Fourier Transform Circuits and Applications to Quantum Metrology

Zu-En Su,[1,2] Yuan Li,[1,2] Peter P. Rohde,[4] He-Liang Huang,[1,2,3] Xi-Lin Wang,[1,2] Li Li,[1,2] Nai-Le Liu,[1,2] Jonathan P. Dowling,[5] Chao-Yang Lu,[1,2] and Jian-Wei Pan[1,2]

[1]*Hefei National Laboratory for Physical Sciences at Microscale and Department of Modern Physics, University of Science and Technology of China, Hefei, Anhui 230026, China*

[2]*CAS Centre for Excellence and Synergetic Innovation Centre in Quantum Information and Quantum Physics, University of Science and Technology of China, Hefei, Anhui 230026, China*

[3]*Henan Key Laboratory of Quantum Information and Cryptography, Zhengzhou Information Science and Technology Institute, Zhengzhou, Henan 450000, China*

[4]*Centre for Quantum Software & Information (QSI), Faculty of Engineering & Information Technology, University of Technology Sydney, Sydney, New South Wales 2007, Australia*

[5]*Hearne Institute for Theoretical Physics and Department of Physics & Astronomy, Louisiana State University, Baton Rouge, Louisiana 70803, USA*

(Received 28 May 2017; published 24 August 2017)

Quantum Fourier transforms (QFTs) have gained increased attention with the rise of quantum walks, boson sampling, and quantum metrology. Here, we present and demonstrate a general technique that simplifies the construction of QFT interferometers using both path and polarization modes. On that basis, we first observe the generalized Hong-Ou-Mandel effect with up to four photons. Furthermore, we directly exploit number-path entanglement generated in these QFT interferometers and demonstrate optical phase supersensitivities deterministically.

DOI: 10.1103/PhysRevLett.119.080502

Quantum interference lies at the heart of quantum mechanics. Increasing the number of single photons and the complexity of optical circuits are key advances for a quantum advantage in many photonic quantum processing tasks [1], including quantum computing [2], quantum simulation [3], and quantum metrology [4].

The Hong-Ou-Mandel (HOM) effect [5] is regarded as one of the quintessential quantum interference phenomena. In the original experiment, two identical single photons interfered and bunched in a two-mode quantum Fourier transform (QFT) interferometer (i.e., a balanced beam splitter). Generally, n identical single photons interfering in an n-mode QFT interferometer [6] will lead to a higher-dimensional bunching effect [7,8], which is expected to play an important role in understanding and exploiting multiphoton interference. A recent application of the QFT is to use it for stringent and efficient assessment of boson sampling [9], which can guarantee the results contain genuine quantum interference [10]. The QFT interferometer has been constructed on chip with up to eight modes [11]. However, only three-photon assessment was demonstrated [12], due in part to the relatively high loss of the optical circuit. For this scheme to work with more photons, it is essential to construct large-scale and low-loss QFT interferometers.

Quantum metrology is another important application intimately related to quantum interference. One of the most versatile quantum metrology devices—the Mach-Zehnder interferometer (MZI), is made up of two balanced beam splitters. Naturally, m-mode QFT interferometers were proposed to construct multimode MZIs for precision improvement [13,14] or the simultaneous estimation of multiple phases [15,16]. Recently, Motes and Olson *et al.* [17,18] pointed out that an n-mode MZI fed with a single photon into each arm can be used to beat the shot noise limit (SNL) deterministically (see Fig. 1), requiring neither nonlinear nor probabilistic preparation of entanglement. However, since multimode MZIs consist of a QFT and an inverse QFT interferometer, having higher loss and lower stability than a single QFT interferometer, only one [13] and two [14] photons have been tested in a three-mode MZI so far. It remains a challenge to observe multiphoton interference in multimode MZIs to beat the SNL.

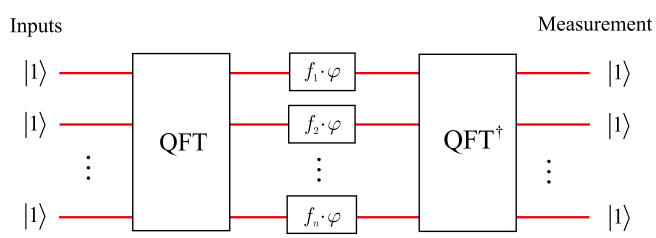

FIG. 1. Quantum metrology scheme of the QFT interferometers using single-photon inputs. The QFT acts as the number-path entanglement generator, while the inverse transform QFT† is used for unentangling the probe. Counting coincidence events with one photon per output mode leads to the probability distribution that is used to estimate the unknown phase φ.

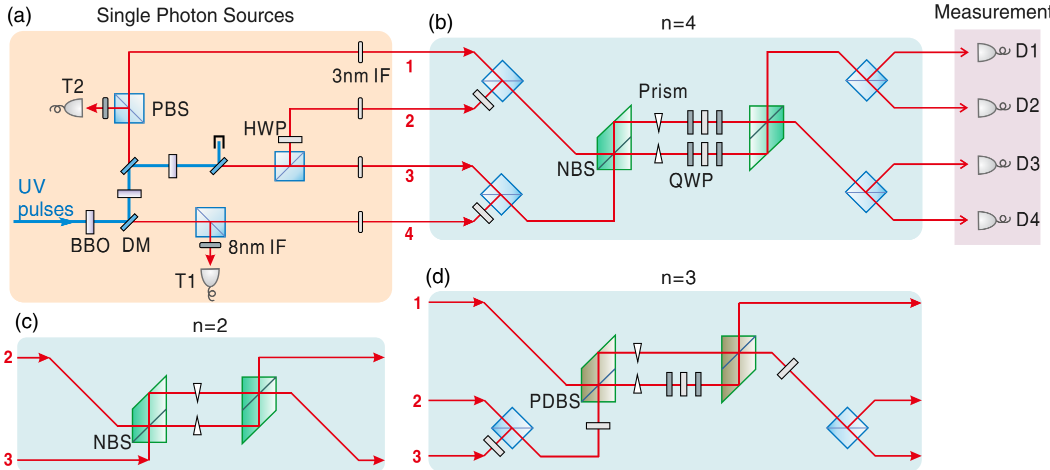

FIG. 2. Experimental setup. (a) The single photon sources. Photons are produced in three nonlinear crystals (BBO) via spontaneous parametric down-conversion. Motorized translation stages Δd_1–Δd_3 (not drawn in the figure) were used to synchronize the delays among paths 1 to 4. The quantum metrology optical circuit with (b) four, (c) two, and (d) three single-photon inputs. The labels are as follow: DM, dichroic mirror, PBS, polarizing beam splitter, PDBS, polarization-dependent beam splitter, NBS, nonpolarizing beam splitter, HWP (QWP), half (quarter) wave plate, Prism, used as the phase shifter between different paths, IF, interferential filter, D1, D2, D3, D4, T1, and T2, fiber-coupled single-photon detectors.

In this work, we develop a general approach to simplifying the construction of QFT interferometers using both path and polarization modes, which makes it possible to reduce resources as much as 75% when compared to devices using only path modes. We report the first experimental demonstration of the generalized HOM effect with up to four photons. Moreover, we constructed multimode MZIs using two cascaded QFTs and observed phase supersensitivities deterministically.

The single-photon inputs were generated via three spontaneous parametric down-conversion (SPDC) sources [Fig. 2(a)], each emitting one pair of photons $|H\rangle_s|V\rangle_i$,

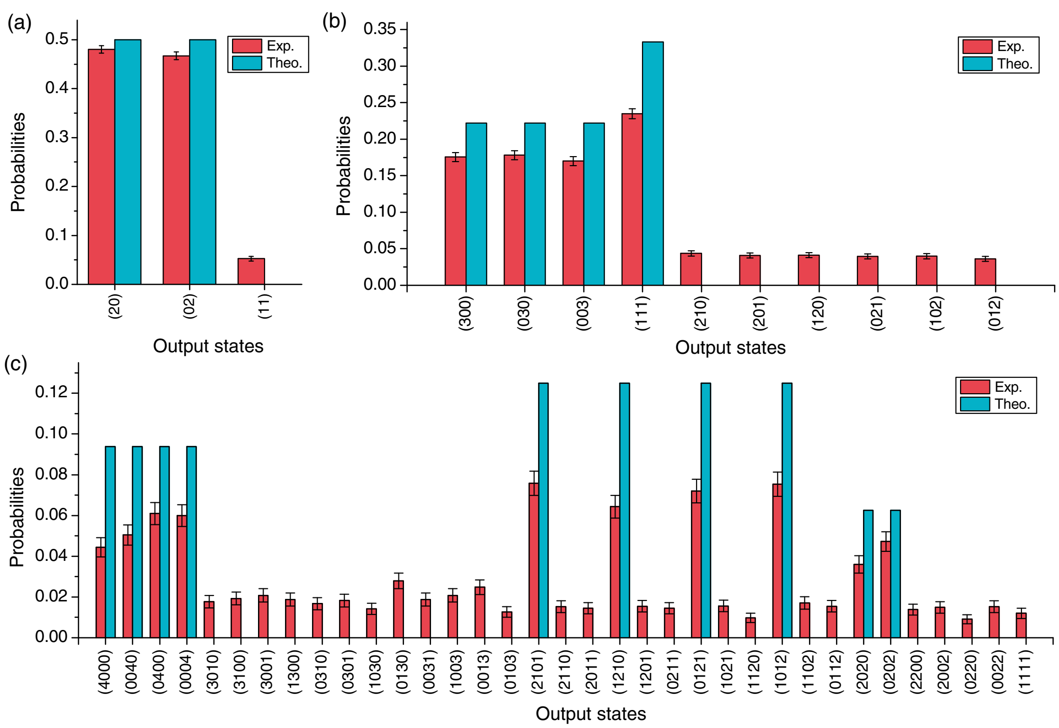

FIG. 3. Experimental results of the generalized HOM effect. (a) $n = 2$, (b) $n = 3$, (c) $n = 4$. These bunching output states with photon number ≥ 2, such as (300) and (210), were measured by multiplexing the single-photon detectors with arrays of beam splitters. Error bars are 1 standard deviation due to propagated Poissonian statistics.

where H and V denote horizontal and vertical polarizations, and s and i correspond to the signal and idler path modes, respectively. For $n = 2$, one pair of SPDC photons was enough, while for $n = 3$, another SPDC was added, and all three SPDCs were used for $n = 3$. For the latter two cases, postselection of a fourfold (sixfold) coincidence, consisting of one (two) triggers, ensures that only three (four) photons enter the setup in separate modes with a negligible higher-order noise.

The QFT interferometers were constructed with low-loss bulk-optical elements. In order to decrease the number of beam splitters and improve the interference stability, we exploited polarization and path modes simultaneously. This simplification enables us to construct the QFT interferometers with only one nonpolarizing beam splitter for $n = 4$ and 2 [Figs. 2(b) and 2(c)], and one polarization-dependent beam splitter for $n = 3$ [Fig. 2(d)]. More details can be found in the Supplemental Material [19].

Generalized HOM effect.—Going through the QFT interferometers, the single-photon inputs will evolve as,

$$|11\rangle \to (|20\rangle - |02\rangle)/\sqrt{2}, \tag{1}$$

$$|111\rangle \to \frac{\sqrt{2}}{3}(|300\rangle + |030\rangle + |003\rangle) - \frac{1}{\sqrt{3}}|111\rangle, \tag{2}$$

$$\begin{aligned}|1111\rangle \to & \frac{\sqrt{6}}{8}(|4000\rangle - |0400\rangle + |0040\rangle - |0004\rangle) \\ & + \frac{\sqrt{2}}{4}(|1210\rangle - |2101\rangle + |1012\rangle - |0121\rangle) \\ & - \frac{1}{4}(|2020\rangle - |0202\rangle).\end{aligned} \tag{3}$$

Other terms are destructively interfered to zero according to the so-called zero-transmission law [7], which predicts which output configurations will be strictly suppressed in the generalized HOM effect. The theoretical and experimental probability distributions are shown in Fig. 3. We use the fidelity defined as $F = \sum_i \sqrt{p_i q_i}$ to quantify the similarity between the experimental probability distribution $\{p_i\}$ and the theoretical one $\{q_i\}$, with respect to the three states in Eqs. (1)–(3). We obtained fidelities of 0.973 ± 0.001, 0.871 ± 0.004, and 0.765 ± 0.008 for $n = 2$, 3, and 4, respectively. To distinguish an effect associated with classical particles, we calculated the experimental violation of Eqs. (1)–(3) as $\upsilon_n = N_s/N_t$, the ratio of the number of predicted suppressed events N_s to the total number of events N_t. For $n = 2$, 3, and 4, the violations with indistinguishable single photons are $\upsilon_2^{\mathrm{ind}} = 0.052 \pm 0.001$, $\upsilon_3^{\mathrm{ind}} = 0.24 \pm 0.01$, $\upsilon_4^{\mathrm{ind}} = 0.41 \pm 0.03$, compared with the larger values $\upsilon_2^{\mathrm{d}} = 0.47 \pm 0.01$, $\upsilon_3^{\mathrm{d}} = 0.68 \pm 0.08$, $\upsilon_4^{\mathrm{d}} = 0.75 \pm 0.14$ with distinguishable single photons (coherent states). (See more details in the Supplemental Material [19].)

The results can also be viewed as a nonclassicality witness of the input sources [8]. We calculated the average second-order correlation function, defined as $\bar{G}_n = \{2/[n(n-1)]\} \sum_{i<j} n_i n_j p_{ij}$, where n_i is the photon number in the ith mode and p_{ij} is the coincidence probability between the ith and jth modes. We obtained $\bar{G}_2 = 0.052 \pm 0.005$, $\bar{G}_3 = 0.396 \pm 0.007$, and $\bar{G}_4 = 0.556 \pm 0.011$, significantly violating their corresponding classical lower bounds $(1 - 1/n)$, $G_2 = 0.5$, $G_3 = 0.67$, $G_4 = 0.75$, and indicating good average pairwise indistinguishability of the input sources.

Quantum metrology based on the QFT.—Our scheme has different phase distributions $\{f_j \varphi\}_{j=1}^n$, as illustrated in Fig. 1. To demonstrate the basic principle, we chose two phase distributions (linear phase $f_j^{\mathrm{lin}} = j - 1$ and delta phase $f_j^{\delta} = \delta_{j,1}$) and implemented two- to four-photon experiments. As shown in Fig. 4, all experimental fringes exhibit phase superresolution and, most importantly, oscillate with a better visibility than the corresponding classically limited

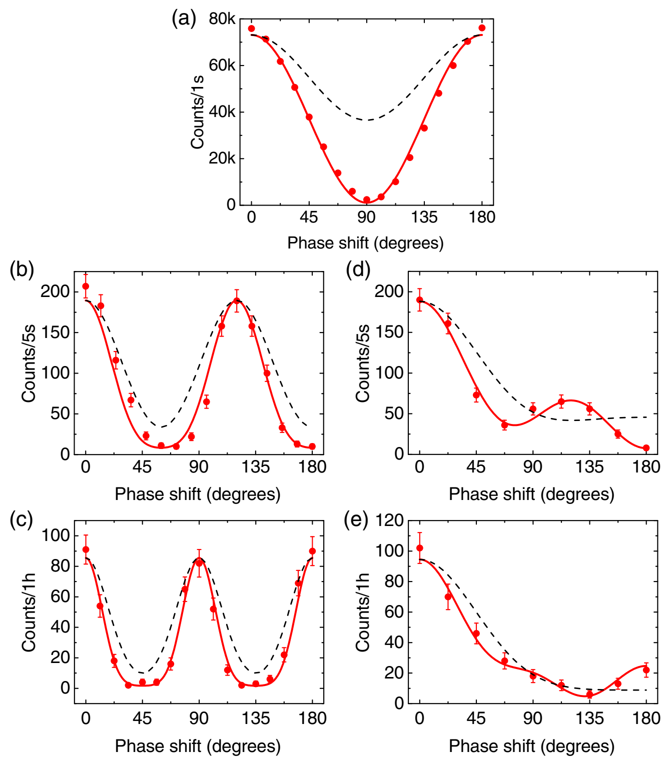

FIG. 4. Measuring counts as function of the phase shift φ for (a)–(c) linear and (d), (e) delta phase distribution. The fringes exhibit 1, 1.5, and 2 distinct oscillations within a half phase cycle for (a) $n = 2$, (b),(d) $n = 3$ and (c),(e) $n = 4$, respectively. Error bars are 1 standard deviation due to propagated Poissonian statistics. The solid red line is a fit to the case of indistinguishable single photons, while the dashed line is the limiting distribution of distinguishable single photons. From (a) to (e), the experimental (classical-limit) visibilities are 0.97 ± 0.02 (0.50), 0.908 ± 0.020 (0.609), 0.962 ± 0.025 (0.790), 0.927 ± 0.037 (0.636), 0.919 ± 0.045 (0.829), respectively. Here, visibility is defined as $(\mathrm{Counts}_{\max} - \mathrm{Counts}_{\min})/(\mathrm{Counts}_{\max} + \mathrm{Counts}_{\min})$, different from the fitted parameter called effective visibility in the main text and the Supplemental Material [19].

TABLE I. Measuring phase sensitivity $\Delta\varphi$ against the number of photons n. Here, HL denotes the Heisenberg limit.

Photon number (n)	$\Delta\varphi_{\text{ideal}}$	$\Delta\varphi_{\text{exp}}$	SNL	HL
2	0.500	0.515 ± 0.013	0.707	0.500
3	0.433	0.491 ± 0.015	0.577	0.333
4	0.408	0.458 ± 0.027	0.500	0.250

distributions, which are given in the Supplemental Material [19]. Different from other schemes based on engineered entangled states, e.g., the N00N state [29], the QFT-based quantum metrology scheme directly exploits deterministically generated entanglement [Eqs. (1)–(3)]. Thus, we do not need to worry about postselection efficiency when trying to demonstrate phase supersensitivity [30].

The linear phase scheme has a phase sensitivity that scales as $O(1/n^{3/2})$ [17]. Unfortunately, the high sensitivity is due to the linearly increasing phase shift $\{(j-1)\varphi\}_{j=1}^{n}$, but not the quantum nature of multiphoton interference [31]. Nevertheless, the linear scheme is superresolving and could have applications to quantum microscopy [32]. Note that the largest relative phase shift is $(n-1)\varphi \sim n\varphi$. If we run a classical two-mode MZI n times to measure the largest relative phase shift $n\varphi$, its classical sensitivity is $\Delta(n\varphi) = O(1/n^{1/2})$, which means $\Delta(\varphi) = O(1/n^{3/2})$, giving the same improvement as the linear phase scheme. In fact, it has been pointed out that Kitaev's phase-estimation algorithm, based on the QFT with a similar linearly increasing phase shift, cannot beat the SNL unless one uses adaptive measurements [33].

The delta function proved to be the best phase distribution to demonstrate phase supersensitivity, although $\Delta\varphi$ only scales as $\sqrt{\{n/[8(n-1)]\}}$ [18]. As the number of photons increases, the phase sensitivity approaches a constant. As a result, the superresolution disappears and the output fringes approach the SNL distribution quickly. Only in the low-photon-number regime ($n \leq 6$) is it possible to beat the SNL. In the experiment, the effective visibilities of the measured fringes are 0.94 ± 0.02 and 0.97 ± 0.03 for $n = 3$ and 4, respectively. They are greater than the corresponding thresholds (0.83 and 0.93) to beat the SNL. As shown in Table I, all the measuring phase sensitivities beat the SNLs. More details can be found in the Supplemental Material [19].

In conclusion, we have experimentally demonstrated the generalized HOM effect in QFT interferometers and observed phase supersensitivities in the multimode MZIs with two, three, and four photons. Our simple QFT devices may be used to realize other QFT-based applications, such as quantum-enhanced multiphase estimation [15,16], entanglement generation and transformation [34], sorting quantum systems efficiently [35], nonmonotonic quantum-to-classical transitions [36], and simulations of a geometric phase [37]. Additionally, the scheme using both path and polarization modes is also suited to optical waveguide systems for simplifying the construction of QFT interferometers.

This work was supported by the National Natural Science Foundation of China (Grant No. 91336214), the Chinese Academy of Sciences, and the National Fundamental Research Program. J. P. D. would like to acknowledge support from the U.S. National Science Foundation. P. P. R. is funded by an ARC Future Fellowship (Project No. FT160100397). All the authors would like to acknowledge Chenglong You, Sushovit Adhikari, Jonathan Olson, and Tim Byrnes for helpful discussions.

[1] J.-W. Pan, Z.-B. Chen, C.-Y. Lu, H. Weinfurter, A. Zeilinger, and M. Żukowski, Rev. Mod. Phys. **84**, 777 (2012).
[2] A. Steane, Proc. R. Soc. A **452**, 2551, 1996; E. Knill, R. Laflamme, and G. J. Milburn, Nature (London) **409**, 46 (2001); P. Kok, W. J. Munro, K. Nemoto, T. C. Ralph, J. P. Dowling, and G. J. Milburn, Rev. Mod. Phys. **79**, 135 (2007).
[3] A. Aspuru-Guzik and P. Walther, Nat. Phys. **8**, 285 (2012); I. Georgescu, S. Ashhab, and F. Nori, Rev. Mod. Phys. **86**, 153 (2014).
[4] H. Lee, P. Kok, and J. P. Dowling, J. Mod. Opt. **49**, 2325 (2002); V. Giovannetti, S. Lloyd, and L. Maccone, Nat. Photonics **5**, 222 (2011).
[5] C. K. Hong, Z. Y. Ou, and L. Mandel, Phys. Rev. Lett. **59**, 2044 (1987).
[6] M. Żukowski, A. Zeilinger, and M. A. Horne, Phys. Rev. A **55**, 2564 (1997); A. Vourdas and J. A. Dunningham, Phys. Rev. A **71**, 013809 (2005); Y. L. Lim and A. Beige, New J. Phys. **7**, 155 (2005).
[7] M. C. Tichy, M. Tiersch, F. de Melo, F. Mintert, and A. Buchleitner, Phys. Rev. Lett. **104**, 220405 (2010); N. Spagnolo, C. Vitelli, L. Aparo, P. Mataloni, F. Sciarrino, A. Crespi, R. Ramponi, and R. Osellame, Nat. Commun. **4**, 1606 (2013).
[8] L. Rigovacca, C. Di Franco, B. J. Metcalf, I. A. Walmsley, and M. S. Kim, Phys. Rev. Lett. **117**, 213602 (2016).
[9] M. C. Tichy, K. Mayer, A. Buchleitner, and K. Mølmer, Phys. Rev. Lett. **113**, 020502 (2014).
[10] M. C. Tichy, J. Phys. B **47**, 103001 (2014).
[11] A. Crespi, R. Osellame, R. Ramponi, M. Bentivegna, F. Flamini, N. Spagnolo, N. Viggianiello, L. Innocenti, P. Mataloni, and F. Sciarrino, Nat. Commun. **7**, 10469 (2016).
[12] J. Carolan, C. Harrold, C. Sparrow, E. Martín-López, N. J. Russell, J. W. Silverstone, P. J. Shadbolt, N. Matsuda, M. Oguma, M. Itoh *et al.*, Science **349**, 711 (2015).
[13] G. Weihs, M. Reck, H. Weinfurter, and A. Zeilinger, Opt. Lett. **21**, 302 (1996).
[14] Z. Chaboyer, T. Meany, L. Helt, M. J. Withford, and M. Steel, Sci. Rep. **5**, 9601 (2015).
[15] P. C. Humphreys, M. Barbieri, A. Datta, and I. A. Walmsley, Phys. Rev. Lett. **111**, 070403 (2013).
[16] M. A. Ciampini, N. Spagnolo, C. Vitelli, L. Pezzè, A. Smerzi, and F. Sciarrino, Sci. Rep. **6**, 28881 (2016);

M. Szczykulska, T. Baumgratz, and A. Datta, Adv. Phys.: X **1**, 621 (2016).
[17] K. R. Motes, J. P. Olson, E. J. Rabeaux, J. P. Dowling, S. J. Olson, and P. P. Rohde, Phys. Rev. Lett. **114**, 170802 (2015).
[18] J. P. Olson, K. R. Motes, P. M. Birchall, N. M. Studer, M. LaBorde, T. Moulder, P. P. Rohde, and J. P. Dowling, Phys. Rev. A **96**, 013810 (2017).
[19] See Supplemental Material at http://link.aps.org/supplemental/10.1103/PhysRevLett.119.080502 for single-photon source characterization, optical interferometer construction, simplifying QFT interferometers using path and polarization modes, classical probability distributions of the QFT interferometers, normalized linear phase versus delta phase, phase sensitivity calculation, and more discussion of Fig. 4, which includes Refs. [20–28].
[20] J. W. Cooley and J. W. Tukey, Math. Comput. **19**, 297 (1965).
[21] G. Strang, Bull. Am. Math. Soc. **28**, 288 (1993).
[22] M. Reck, A. Zeilinger, H. J. Bernstein, and P. Bertani, Phys. Rev. Lett. **73**, 58 (1994).
[23] W. R. Clements, P. C. Humphreys, B. J. Metcalf, W. S. Kolthammer, and I. A. Walsmley, Optica **3**, 1460 (2016).
[24] P. Törmä, I. Jex, and S. Stenholm, J. Mod. Opt. **43**, 245 (1996).
[25] R. Barak and Y. Ben-Aryeh, J. Opt. Soc. Am. B **24**, 231 (2007).
[26] G. Tabia, Phys. Rev. A **93**, 012323 (2016).
[27] E. Poem, Y. Gilead, and Y. Silberberg, Phys. Rev. Lett. **108**, 153602 (2012).
[28] A. Peruzzo, A. Laing, A. Politi, T. Rudolph, and J. L. O'brien, Nat. Commun. **2**, 224 (2011).
[29] A. N. Boto, P. Kok, D. S. Abrams, S. L. Braunstein, C. P. Williams, and J. P. Dowling, Phys. Rev. Lett. **85**, 2733 (2000); J. P. Dowling, Contemp. Phys. **49**, 125 (2008).
[30] K. J. Resch, K. L. Pregnell, R. Prevedel, A. Gilchrist, G. J. Pryde, J. L. O'Brien, and A. G. White, Phys. Rev. Lett. **98**, 223601 (2007); T. Nagata, R. Okamoto, J. L. O'Brien, K. Sasaki, and S. Takeuchi, Science **316**, 726 (2007).
[31] G. M. D'Ariano and M. G. A. Paris, Phys. Rev. A **55**, 2267 (1997); J. Söderholm, G. Björk, B. Hessmo, and S. Inoue, Phys. Rev. A **67**, 053803 (2003); J. Chwedeńczuk, F. Piazza, and A. Smerzi, Phys. Rev. A **87**, 033607 (2013).
[32] T. Juffmann, B. B. Klopfer, T. L. Frankort, P. Haslinger, and M. A. Kasevich, Nat. Commun. **7**, 12858 (2016).
[33] B. L. Higgins, D. W. Berry, S. D. Bartlett, H. M. Wiseman, and G. J. Pryde, Nature (London) **450**, 393 (2007); V. Giovannetti, S. Lloyd, and L. Maccone, Phys. Rev. Lett. **96**, 010401 (2006).
[34] Y. L. Lim and A. Beige, Phys. Rev. A **71**, 062311 (2005).
[35] R. Ionicioiu, Sci. Rep. **6**, 25356 (2016).
[36] M. C. Tichy, H.-T. Lim, Y.-S. Ra, F. Mintert, Y.-H. Kim, and A. Buchleitner, Phys. Rev. A **83**, 062111 (2011); Y.-S. Ra, M. C. Tichy, H.-T. Lim, O. Kwon, F. Mintert, A. Buchleitner, and Y.-H. Kim, Proc. Natl. Acad. Sci. U.S.A. **110**, 1227 (2013).
[37] A. Laing, T. Lawson, E. Martín López, and J. L. O'Brien, Phys. Rev. Lett. **108**, 260505 (2012).